Eur. Phys. J. D **24**, 53–56 (2003)
DOI: 10.1140/epjd/e2003-00105-x

THE EUROPEAN PHYSICAL JOURNAL D

Vibrational spectroscopy of large water clusters of known size

P. Andersson[a], C. Steinbach, and U. Buck[b]

Max–Planck–Institut für Strömungsforschung, 37073 Göttingen, Germany

Received 10 September 2002
Published online 3 July 2003 –

Abstract. The structure of large water clusters of known size distributions $\langle n \rangle = 20-2000$ is investigated by vibrational spectroscopy of the OH stretch mode. The water clusters are predissociated by a pulsed tunable infrared optical parametrical oscillator (OPO) in the frequency range 2800−3800 cm^{-1}. Their fragments are detected off-axis by electron impact ionization and mass analyzed by a quadrupole mass spectrometer. The largest ion signal stems from the neutral water hexamer fragment. The ion yield is investigated at certain wavelengths while the size of the clusters is varied, and for certain sizes complete absorption spectra of the OH stretch motion are measured. Fingerprints of the different coordination types of the water molecules in the clusters are found and it turns out that our method is especially sensitive to amorphous structures with frequencies shifting in the range of 3300−3400 cm^{-1}.

PACS. 36.40.Mr Spectroscopy and geometrical structure of clusters – 61.46.+w Nanoscale materials: clusters, nanoparticles, nanotubes, and nanocrystals

1 Introduction

The condensed phase of water still attracts much interest for different reasons. On the one hand, water plays a key role as solvent and as promotor of reactions in terrestrial, atmospheric, and extraterrestrial chemistry. On the other hand, the numerous anomalous physical properties of the liquid and solid bulk water make this hydrogen bonded network so interesting [1]. However, a unified description of bulk water starting from the basic molecular interaction is still missing, since the hydrogen bonds are caused by strong oriented forces that are difficult to model theoretically. Therefore water clusters provide an appropriate tool for two reasons. First, variation of the cluster size allows to investigate experimentally the development of macroscopic properties of the bulk step by step. Second, the finite number of particles in a defined environment makes their theoretical treatment easier than that of the bulk.

Vibrational spectroscopy of the OH stretch mode is a sensitive indicator of the strength and coordination of the hydrogen bond [2]. This mode is shifted in the network of the clusters up to 800 cm^{-1} to the red, compared to the vibrational stretch modes of the water molecule, the symmetric one at 3655 cm^{-1}, and the asymmetric one at 3756 cm^{-1}, respectively.

For small, 3-dimensional water clusters in the size range $n = 6-10$ various size selective spectroscopic experiments have been carried out [3–11]. The resulting structures can be derived from the octamer cube by adding or subtracting molecules, and characteristic fingerprints of the different coordination types of the hydrogen bonds can be found in the vibrational spectra.

For larger clusters, only data are available where the sizes are not known. Aside from the isolated peak of the free OH stretch at 3720 cm^{-1}, mainly broad distributions were measured [12–16]. Furthermore, Fourier Transform Infrared (FTIR) measurements of even larger ice nanoparticles were carried out [17–19].

The IR spectrum of liquid water, finally, shows a broad, unstructured distribution with a maximum at 3450 cm^{-1} [20], whereas the spectrum of hexagonal ice exhibits a somewhat less broad distribution, peaked at 3220 cm^{-1} with shoulders at 3100 cm^{-1} and 3380 cm^{-1} [21]. Here, the redshift is an indication of the stronger hydrogen bonds in the solid, while the width of the distributions can be traced back to proton disorder [22].

In the present study large water clusters of known size distributions are produced and their size dependent OH stretch spectra are measured by fragment spectroscopy.

2 Experiment

Large water clusters in the size range of $\langle n \rangle = 20-2000$ are produced in a supersonic expansion of pure water vapor. To obtain information about the size distribution the cluster beam crosses a pick–up cell with sodium of 0.23 Pa

[a] *Present address:* Department of Chemistry, Physical Chemistry, Göteborg University, 412 96 Göteborg, Sweden.
[b] e-mail: ubuck@gwdg.de

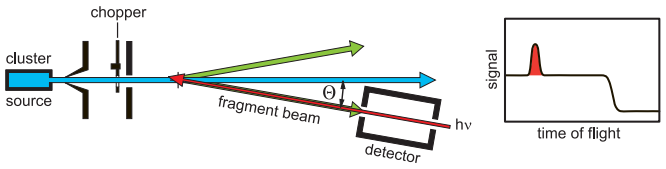

Fig. 1. Schematic view of the experimental set–up.

vapor pressure. Thus the clusters are doped by one sodium atom and thereby accessible for photoionization free of fragmentation. This is caused, on the one hand, by a substantial decrease of the ionization potential (IP) of the $Na(H_2O)_n$ clusters to constantly 3.2 eV for $n \geq 4$ [23], which can easily be reached by photons of a pulsed excimer laser pumped dye laser. Thus they can be ionized at the threshold with a wavelength of 388 nm. On the other hand, the neutral and ionic potential curves of the Na doped water clusters do not differ very much, so there is a high Franck–Condon overlap between the low vibrational levels of the neutral and ionic groundstates, respectively. Thereby no additional energy is deposited in the resulting $(H_2O)_nNa^+$ ions. Thus their distribution, measured in a reflectron time–of–flight mass spectrometer (RETOF-MS), represents the size distribution of the pure, neutral water cluster beam [24].

The vibrational spectra of the large $(H_2O)_n$ clusters are measured in another machine [25]. The schematic experimental arrangement is depicted in Figure 1. The detector, a rotatable quadrupole mass filter with a continuous electron bombardment ion source, is positioned at an angle Θ of about 2−4.5° with respect to the water cluster beam. A chopper allows digital lock–in (DLI) measurements, to discriminate the signal of the continuous water cluster beam from background. The pulsed infrared OPO output crosses the cluster beam under the same angle, and is tuned in a frequency range of 2800−3800 cm^{-1} with a bandwidth of 0.2 cm^{-1}. If a vibrational mode of the clusters is excited, the energy is redistributed and leads to the decay of the clusters, which is, however, not unimolecular. Neutral units of up to seven water molecules are leaving the clusters and thereby the direction of the water cluster beam. Therefore they are detected as enhancement following the laser pulse in the time resolved ion signal of the corresponding masses. We note, that, for simple energetical reasons, two infrared photons are necessary to dissociate the large clusters and to form the mentioned subunits.

3 Results and analysis

The pulsed infrared radiation excites vibrational modes of the water clusters, which results in the decay by predissociation. The outcoming fragments leave the direction of the direct water cluster beam and are detected by electron bombardment ionization. First, we measured the angular distribution of the different fragments, as well as their relative intensities. The mean cluster size of the water cluster beam was $\langle n \rangle = 300$, and the IR wavenumber

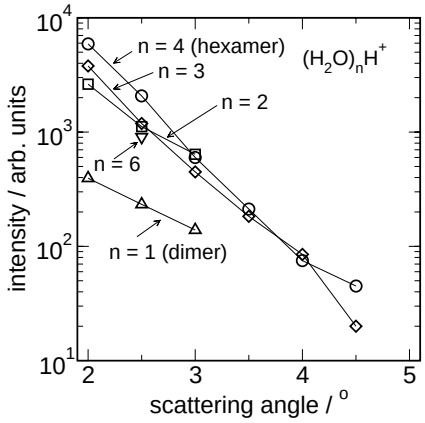

Fig. 2. Angular dependence of the indicated ion signals at a mean cluster size of $\langle n \rangle = 300$ at a wavelength of 3718 cm^{-1} (free OH). In brackets the most probable neutral precursors of the ions are denoted.

was 3718 cm^{-1}, which excites the free OH stretch motion of the water clusters. The result is depicted in Figure 2. It can be seen that the falloff of the ion signal is getting steeper with increasing mass. This is caused by kinematical reasons, since, the heavier the corresponding neutral fragments are, the smaller their velocity perpendicular to the original direction of the mother cluster will be. The absolute intensity of $(H_2O)_4H^+$ is at small angles by far the largest, especially compared to $(H_2O)H^+$. We attribute these ions, because of fragmentation, to the neutral hexamer and dimer, respectively [26].

Now we measured complete vibrational predissociation spectra for different mean cluster sizes in the frequency range of 2800−3800 cm^{-1}. Furthermore, using differently shaped nozzles, we varied the temperature of the water clusters. We note that the amplitudes in these measurements do not necessarily reflect the IR absorption cross sections. They are the product of these with the coupling of the respective intramolecular motions to intermolecular excitation along the H bonds. Those finally lead to the dissociation of the clusters [27]. All the measurements were carried out at the mass of the fragment ion $(H_2O)_4H^+$, that we attribute to the neutral $(H_2O)_6$. The results are shown in Figure 3. The spectra are dominated by peaks at 3720 cm^{-1}, 3550 cm^{-1}, and a variable one moving from 3420 cm^{-1} to 3350 cm^{-1}. In addition they all exhibit a small shoulder near 3200 cm^{-1}.

Finally we measured the dependence of the $(H_2O)_4H^+$ ion signal from the mean cluster size $\langle n \rangle$ for two different wavelengths, namely 3718 cm^{-1}, corresponding to the free OH stretch motion, and 3200 cm^{-1}, where the 4-fold coordinated molecules absorb. The results for different temperatures are shown in Figure 4. The distributions start at about $\langle n \rangle = 30$, exhibit a pronounced peak around $\langle n \rangle = 65$ and fall off at about $\langle n \rangle = 300$ with a long tail. Here, a difference between the cold and warm clusters is observed. Whereas the intensity of the ion signal drops to nearly zero for the colder clusters, their is still substantial intensity for the warmer ones.

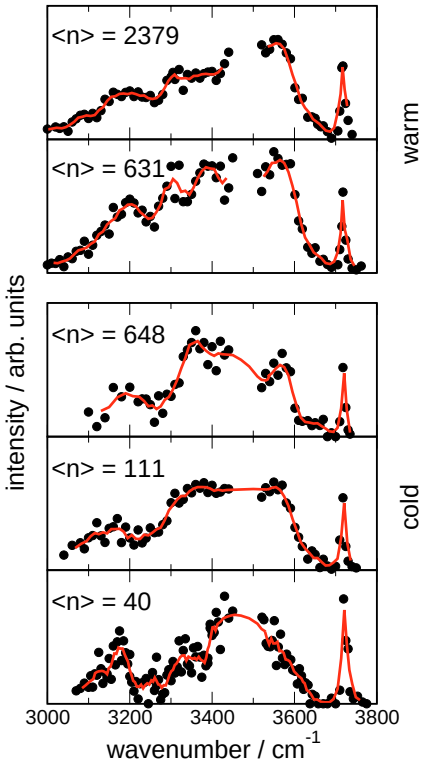

Fig. 3. Measured OH stretch spectra detected at $(H_2O)_4H^+$ for the mean cluster sizes indicated. The spectra were taken at different temperatures.

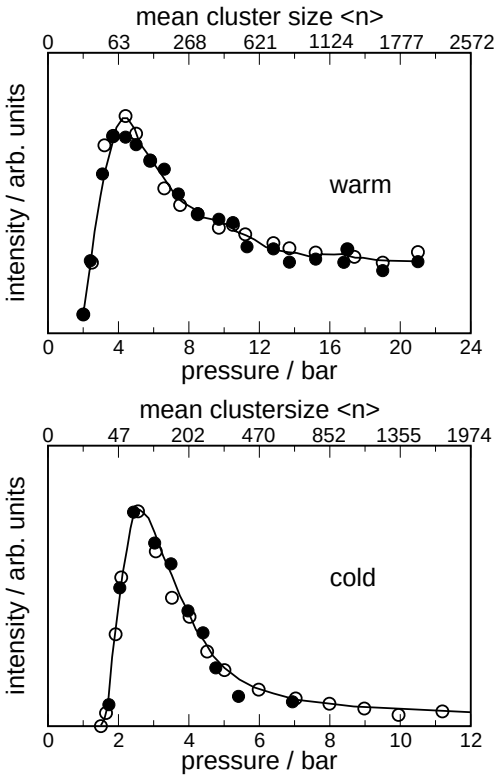

Fig. 4. Cluster size dependence of the OH stretch intensity taken at 3718 cm^{-1} (full circles) and 3200 cm^{-1} (open circles) at the mass $(H_2O)_4H^+$ for different temperatures.

4 Discussion

The OH stretch spectra are measured by detecting the outcoming fragments after the absorption of the IR laser light from a tunable OPO. This has the advantage that also for large clusters the detection is possible without problems compared to the usual depletion technique where the loss of a small fragment is difficult to measure. As can be seen in Figure 2, ion fragments at least up to $(H_2O)_6H^+$ are detected, with $(H_2O)_4H^+$ having the highest intensity. Here original clusters of the mean size $\langle n \rangle = 300$ were irradiated by light of 3718 cm^{-1}. The $(H_2O)_4H^+$ ion fragments are traced back to mainly $(H_2O)_6$ precursors. In earlier experiments, using the same technique [12–14], a different behavior was observed with dominating $(H_2O)H^+$ ion intensities. The main difference here is the size range of the investigated water cluster beams. Scaling laws that we have derived based on measuring size distributions free of fragmentation [24], give mean cluster sizes of $\langle n \rangle \leq 10$ for the source conditions used in these experiments. In this size range the cluster intensities fall exponentially with n. Thus, the predissociation presumably leads to the loss of small entities like monomers and dimers from these small mother clusters. In our case with the log-normal distributions of the large clusters, the detected ions stem from larger units (up to $n = 9$) having left their mother clusters. Apparently there seems to be a preference for pentamer and hexamer units leaving the clusters, thus pointing to already preformed cyclic structures of this kind, as a first indication of amorphous behavior of the mother clusters.

Using differently shaped nozzles, we were able to influence the temperature of the water cluster beams. A smaller effective nozzle diameter has to be compensated by a higher stagnation pressure, using the same nozzle temperature, to produce clusters of the same size. This leads to different relations of pressure and cluster size, as can be observed in Figure 4. The main difference, however, was the length of the conical shaped nozzles. Using 6 mm instead of 2 mm, the beam expands for a substantially longer time, before the zone free of interaction is reached. Therefore the cooling by collisions with the remaining monomers is more effective. Despite of not knowing the exact cluster temperatures, the results obtained with the different nozzles are marked with *warm* and *cold*.

The vibrational spectra shown in Figure 3 are taken at different cluster size distributions and different temperatures. Independent of the mean cluster size, the spectra show peaks at 3718 cm^{-1} and at 3550 cm^{-1}, that can definitely be attributed to the free OH (dangling H) and the double donor single acceptor (DDA, dangling O) molecules at the surface. At 3200 cm^{-1} in all cases the signature of the 4-fold coordinated crystalline ice is found. The interesting part is the maximum at 3400 cm^{-1}, that shifts to smaller frequencies down to 3300 cm^{-1} with increasing cluster size and temperature. We attribute this part of the spectrum to amorphous behavior. The peak of bulk amorphous water is close to 3260 cm^{-1}. However, in the calculation of OH stretch water cluster spectra, this peak is found at 3350 cm^{-1}, and the blue shift is

attributed to the decrease of interior 4-fold coordinated molecules with decreasing cluster size [18]. Obviously, lowering the cluster temperature leads as well to a decrease of these amorphous structured interior molecules, in favor of crystalline structure. The results are in qualitative agreement with those obtained by the same predissociation technique [12–15], although the cluster size is not known in these contributions. The experiments using FTIR [17–19] and cavity ring down [16] spectroscopy show similar features, but with a transition to peaks at 3200 cm^{-1} (corresponding to crystalline ice), that was never observed in the dissociation experiments. The only other attempt to derive size selective information in this size range is that of Devlin and coworkers described in references [17,18]. The result, peak intensities at 3300 cm^{-1} for $\langle n \rangle = 150$ and 3400 cm^{-1} for $\langle n \rangle = 48$ are in reasonable agreement with our results. Again there is a strong indication that we are sensitive to amorphous structures, not only because of the blue shift due to the decrease of the cluster size, but as well because of the red shift of the amorphous peak due to the higher cluster temperature of $\langle n \rangle = 631$ compared to $\langle n \rangle = 648$, as can be seen in Figure 3.

With our ability to provide information about the cluster sizes, we carried out the experiment to determine the range of predominantly amorphous clusters. The results are depicted in Figure 4. We detected again the fragments $(H_2O)_4H^+$ in the range of the free (3718 cm^{-1}) and hydrogen bonded (3200 cm^{-1}) OH stretch frequencies. A pronounced peak around $\langle n \rangle = 65$ is found with a steep falloff to $\langle n \rangle = 300$ followed by a long tail and approaching zero for the cold clusters. If the cluster temperature is raised, the shape of the curve is the same, especially the position of the maximum, but the tail approaches zero much more slowly. This indicates again a preference of our method for the dissociation of amorphous clusters. Presumably the $(H_2O)_n$ clusters start to form a crystalline core at n = 100-300, which gets more dominant with increasing cluster size. Raising the cluster temperature leads to a preponderance of the amorphous fraction.

This work was supported by the Deutsche Forschungsgemeinschaft.

References

1. F. Franks, *Water: A comprehensive Treatise* (Plenum, New York 1972)
2. S.S. Xantheas, T.H. Dunning, *Advances in Molecular Vibrations and Collision Dynamics* (JAI Press, Stamford 1998), p. 281
3. K. Liu, M.G. Brown, C. Carter, R.J. Saykally, J.K. Gregory, D.C. Clary, Nature **381**, 501 (1996)
4. U. Buck, I. Ettischer, M. Melzer, V. Buch, J. Sadlej, Phys. Rev. Lett. **80**, 2578 (1998)
5. J. Brudermann, M. Melzer, U. Buck, J. Kazimirski, J. Sadlej, V. Buch, J. Chem. Phys. **110**, 10649 (1999)
6. R.N. Pribble, T.S. Zwier, Science **265**, 75 (1994)
7. C.J. Gruenloh, J.R. Carney, C.A. Arrington, T.S. Zwier, S.Y. Fredericks, K.D. Jordan, Science **276**, 1678 (1997)
8. T. Watanabe, T. Ebata, S. Tanabe, N. Mikami, J. Chem. Phys. **105**, 408 (1996)
9. W. Roth, M. Schmitt, C. Jacoby, D. Spangenberg, C. Janzen, K. Kleinermanns, Chem. Phys. **239**, 1 (1998)
10. C. Janzen, D. Spangenberg, W. Roth, K. Kleinermanns, J. Chem. Phys. **110**, 9898 (1999)
11. H.D. Barth, K. Buchhold, S. Djafari, B. Reimann, U. Lommatzsch, B. Brutschy, Chem. Phys. **239**, 49 (1998)
12. M.F. Vernon, D.J. Krajnovich, H.S. Kwok, J.M. Lisy, Y.R. Shen, Y.T. Lee, J. Chem. Phys. **77**, 47 (1982)
13. R.H. Page, J.G. Frey, Y.R. Shen, Y.T. Lee, Chem. Phys. Lett. **106**, 373 (1984)
14. R.H. Page, M.F. Vernon, Y.R. Shen, Y.T. Lee, Chem. Phys. Lett. **141**, 1 (1987)
15. F. Huisken, S. Mohammed-Pooran, O. Werhahn, Chem. Phys. **239**, 11 (1998)
16. J.B. Paul, C.P. Collier, R.J. Saykally, J.J. Scherer, A.O. O'Keefe, J. Phys. Chem. **101**, 5211 (1997)
17. J.P. Devlin, C. Joyce, V. Buch, J. Phys. Chem. A **104**, 1974 (2000)
18. V. Buch, J.P. Devlin, in *Water in confined geometries* (Springer, Heidelberg, 2003)
19. L.Goss, S.W. Sharpe, T.A. Blake, V. Vaida, J.W. Brault, J. Phys. Chem. A **103**, 103 (1999)
20. G.E. Walrafen, J. Chem. Phys. **47**, 114 (1967)
21. M.S. Bergren, D. Schuh, M.G. Sceats, S.A. Rice, J. Chem. Phys. **69**, 3477 (1978)
22. V. Buch, J.P. Devlin, J. Chem. Phys. **110**, 3437 (1999)
23. C.P. Schulz, R. Haugstätter, H.-U. Tittes, I.V. Hertel, Phys. Rev. Lett. **57**, 1703 (1986)
24. C. Bobbert, S. Schütte, C. Steinbach, U. Buck, Eur. Phys. J. D **19**, 183 (2002)
25. U. Buck, F. Huisken, J. Schleusener, J. Schaefer, J. Chem. Phys. **72**, 1512 (1980)
26. U. Buck, M. Winter, Z. Phys. D **31**, 291 (1994)
27. U. Buck, Adv. At. Mol. Opt. Phys. **35**, 121 (1995)